Preparation and Characteristics Study on Ni Substituted Mixed Ferrites

Selvanandan.S[1] and Ramesh.C

[1] Department of Physics, ACS College of Engineering, Kambipura, Mysore Road, Bangalore, Karnataka, India

Department of Mechanical Engineering, Rajarajeshwari College of Engineering, Bangalore,India

ABSTRACT

Ni-substituted MnZn mixed ferrite prepared by conventional sol-gel method. Ni substituted MnZn ferrite of molecular formula $Mn_{0.3}Zn_{0.7}Ni_xFe_{2-x}O_4$ in which five samples of x=0.0, x=0.4, x=0.8, x=1.2 and x=1.6 were prepared. The X-ray intensity of (4 0 0) plane were used to calculate particle size and studied its variation with Nickel concentration. XRD, SEM, FTIR and VSM characteristics were presented. The substitution of Ni by replacing Fe reduces the coercivity of the ferrite due to replacement of Ni^{2+} by Fe^{3+} in tetrahedral site. Infrared spectroscopies have been discussed so as to bring out the role of nickel substitution in determining structural properties of Zn–Mn ferrites and the role of nitrates in preparation of these compounds.

Keywords: Ferrites, Nanopowders, Magnetic materials, XRD, VSM, SEM, FTIR, Magnetic Anisotropy.

1. Introduction

Mixed-ferrite nanoparticles have been intensively studied in the last decade due to their unusual physical and magnetic properties owing to their extremely small size and number of promising applications. A special application of MnZn-ferrites is found in the absorption of radar signals, which is the basis of stealth technology. As a result, numerous applications of metal oxides, such as fabrication of microelectronic circuits, sensors, piezoelectric devices, fuel cells, dielectrics, lasers, magnets and catalysts have been discussed [1–13].

Recently, considerable effort has been made on the surface modification of nanoparticles and the preparation of different types of metal oxides. Various methods are available for the synthesis of metal oxides, such as microwave refluxing [14], sol–gel [15,16], hydrothermal [17,18], co-precipitation [19,20], citrate–gel [21], spray pyrolysis [22], etc. The selection of appropriate synthetic procedure often depends on the desired properties and final applications. Among these synthesis techniques, sol–gel autocombustion method has several advantages over others for preparation of nanosized metal oxides.

[1]Corresponding Author: Selvanandan S, Email:selvanandan@gmail.com; Phone: 8884451258

The addition of dopants mentioned above, while improving some characteristics of MnZn ferrites (reduce the power loss for example), usually brings deterioration of other characteristics (lower the initial permeability), therefore, combination of different dopants are needed to alleviate negative effects [23].

In this paper, small amount of Nickel nitrate is added to replace Iron in MnZn ferrites by sol-gel method. Nickel substitution on magnetic and microstructures of $Mn_{0.3}Zn_{0.7}Ni_xFe_{2-x}O_4$ (x=0.0, x=0.4, x=0.8, x=1.2, x=1.6) were synthesized by a nitrate-citrate precursor method. The structural and magnetic characteristics were studied as function of nickel concentration using XRD, SEM, FTIR and VSM. The relationship between microstructures and magnetic properties of these ferrites were discussed.

2. Experimental procedure

The powders were synthesized by sol-gel auto combustion method. Analytic grade Zinc Nitrate $(Zn(NO_3)_2.6H_2O)$, Nickel Nitrate $(Ni(NO_3).6H_2O)$, Manganese Nitrate $(Mn(NO_3).6H_2O)$, Ferric Nitrate $(Fe(NO_3)_3.9H_2O)$ were dissolved in distilled water to obtain a mixed solution. Reaction procedure was carried out in air atmosphere.

The molar ratio of metal nitrate to citric acid was taken as 1:3. Ammonia solution was slowly added to adjust the pH at 7. The mixed solution was placed in hot plate at 150^oC until the solution becomes brown gel. When finally all molecules were removed from the mixture the viscous gel began fizzing. The as prepared samples were then sintered at 850° C for 5 hours to get ash powders. Then, those powders were grinded using piston and mortar, and these fine powders were again sintered at 1100^oC for 3 hours. The final powder samples were granulated using acetone as binder for to get final product.

The pH value of the mixed solutions were measured by using a PHS-29A meter, X-ray diffraction (XRD) pattern of the ferrite powders were measured using a Rigaku D/Max 2400 X-ray diffractometer with Cu K_α radiation (40kV, 30 mA). The average grain sizes of the powder were estimated from the diffraction peak width through Scherrer's equation [24]. For the Rietveld refinements, the XRD data were recorded from 10° to 60° (2θ) with steps width of 0.02^o and the count time of 0.60 sec per step. The scanning electron micrographs were obtained on JSM-6460 Scanning Electron Microscope. The magnetic properties of the nanopowders were

measured at room temperature by physical properties measurement system (PPMS) equipped with a high accuracy vibrating sample magnetometer (VSM). Fourier Transform Infrared (FTIR) Spectra of samples were detected by BRUKER TENSOR27 FTIR Spectrometer with transmission from 450 to 4000cm^{-1} using KBr pellets.

3. Results and Discussions

The XRD analysis of $Mn_{0.3}Zn_{0.7}Ni_xFe_{2-x}O_4$ samples calcined at room temperature are shown in figure 1. The single crystal spinel $Mn_{0.3}Zn_{0.7}Ni_xFe_{2-x}O_4$ ferrite was formed as the most intense (311) peak of the Fe_2O_4 and all miller indices (111), (200), (311), (400) and (422) matched well with the reflections of Mn-Zn-Ni ferrite reported in the standard JCPDS data card. The intense sharp peak arose with increase in the concentration of nickel indicating poor crystallite at low concentration. Larger the doping content of the nickel the peak width decreases as the crystallites becomes larger. The XRD pattern showed the formation of single phase's cubic spinel structure without any trace of secondary phase.

The lattice constant refers to the content distance between unit cell in a crystal lattice. The lattice constant 'a' was calculated using the relation $a = d/\sqrt{(h^2 + k^2 + l^2)}$ [25].

The 'd' spacing values were calculated for the recorded peaks using Braggs law and the lattice constant 'a' was calculated for each plane and it found that the average lattice constant 'a' for these mixed ferrite system is 8.58 Å This may due to the addition of Ni^{2+} over MnZn Ferrite, Ni tends to occupy tetrahedral site by replacing Fe^{3+}. The particle size of the sample powders was determined by scherrer's equation [24] $D_{hkl} = \frac{0.9\lambda}{B_{hkl}\cos\theta}$. Here, the D_{hkl} was the particle size obtained from the peak with maximum intensity which corresponds to miller indices (311) in all XRD pattern. B_{hkl} was the full width of the peak at half maximum(in radians). The ferrite morphology shown using SEM micrograph in figure (2), indicating that the phase fine powders shows the tendency for agglomeration. It also observed that the grains were composed of very fine particle with size of nanometers indicating that the sol-gel method produces fine powders and tendency for easy sintering. The calculated particle size from XRD and SEM results was given in figure (3).

Figure (4) represents the typical magnetization curve for Ni^{2+} substituted MnZn spinel Ferrite system sintered at 1100^0 C measured at room temperature with

applied field of 1.5 kOe. It observed that the substitution of Ni^{2+} replaced Fe^{3+} in tetrahedral site results in decreasing magnetization. Since Zn nanocrystals have normal spinel structure, all Zn^{2+} fill tetrahedral site. Hence Fe^{3+} ions forced to occupy the entire octahedral site. These distribution calculation for these ferrites are in agreement with the structure[26]. The impact of coercivity on increase of Ni concentration in MnZn ferrite may due to large crystal size of Fe^{3+} ions of radius 0.67 Å were replaced with Ni^{2+} of 0.78 Å promotes sintering and it leads to increase of grain size [27] which was observed in XRD pattern. Larger grains tend to consists of greater number of domain walls. The magnetisation caused by domain wall movement, requires less energy than that required by domain rotation. As the number of domain wall increases with grain size, and hence the samples having grain size expected to have low coercivity [28]. Variation of saturation magnetization and coercivity from VSM is given in figure (5).

The FTIR spectrograph is a very useful technique to deduce the structural investigation and redistribution of cation between octahedral and tetrahedral sites of spinel ferrites. The FTIR spectrum of $Mn_{0.3}Zn_{0.7}Ni_xFe_{2-x}O_4$ nanoparticles is represented in figure (6). IR spectrum recorded from 4000 cm^{-1} – 450 cm^{-1} shows characteristics interaction between oxygen and metal cations of tetrahedral and octahedral Fe-O-Fe stretching band at 550cm^{-1}[29]. All the dried gel shows the characteristics peak at 1600 cm^{-1} & 1350 cm^{-1} corresponding to the carboxyl group and NO_3^- ions respectively. The band about 850 cm^{-1} is also corresponds to the existence of NO_3^- in the citrate gel. Therefore the combustion can be considered as a thermally induced one, redon reaction of the gel where the citrate ion acts as a reductant and nitrate acts as a oxidant.

Conclusion

The Ni substitution MnZn mixed ferrite was synthesized via sol-gel auto combustion method. From the XRD and the SEM images shows that the substitution of Ni on MnZn ferrite increases the crystal size intern increases larger domain walls. Ni^{2+} replaces Fe^{3+} in tetrahedral site results in decrease of saturation magnetization. Larger the domain wall smaller the coercivity due to the increase of Nickel concentration. The role of nitrate in combustion process and influence of Ni^{2+} ions involves in preparation of the compound via sol-gel method was confirmed with FTIR results.
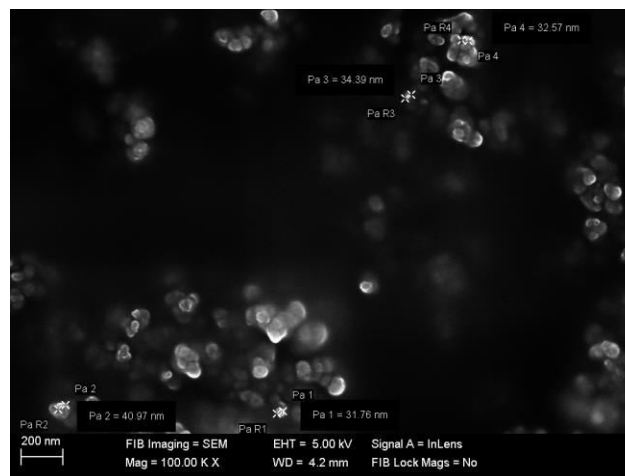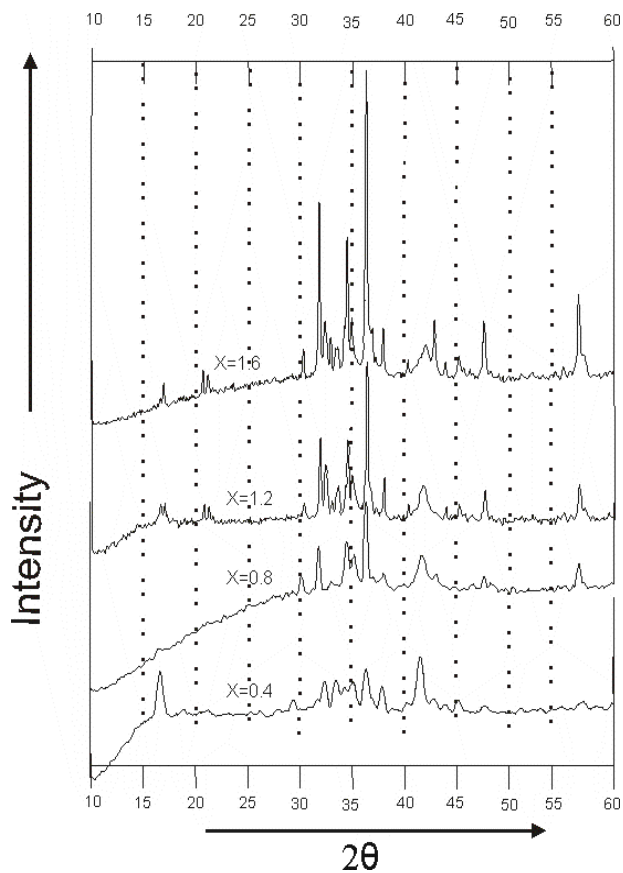
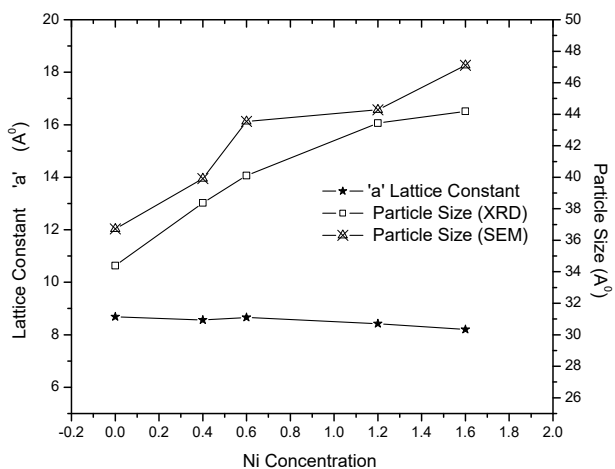Figure (1). XRD pattern of $Mn_{0.3}Zn_{0.7}Ni_xFe_{2-x}O_4$ (x=0.4, x=0.8, x=1.2, x=1.6).
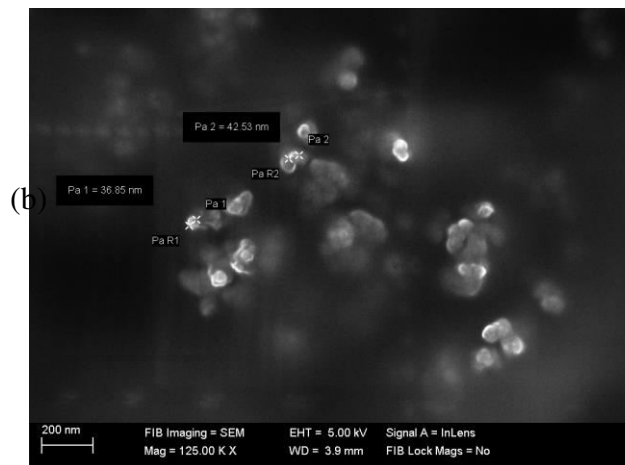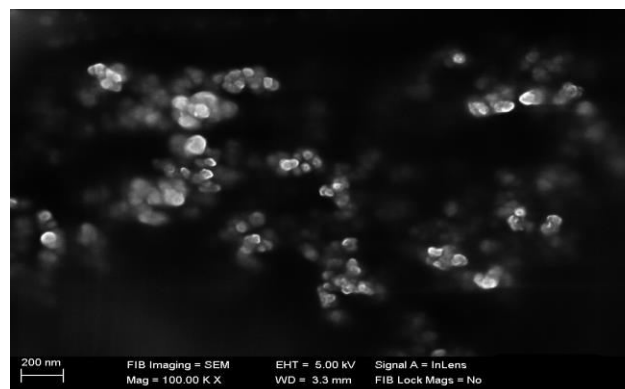

(b)

(c)

Figure (2). Variation of Lattice Constant and crystal size with nickel concentration in $Mn_{0.3}Zn_{0.7}Ni_xFe_{2-x}O_4$ Ferrites.

(a)

(a) x = 0.0, (b) x = 0.4, (c) x = 0.8, (d) x = 1.2,(e) x=.1.6.

(d)

Figure (4). B-H Loop for $Mn_{0.3}Zn_{0.7}Ni_xFe_{2-x}O_4$ Ferrites (x = 0.0(S1), x = 0.4(S2), x = 0.8(S3), x = 1.2(S4), x = 1.6(S5))
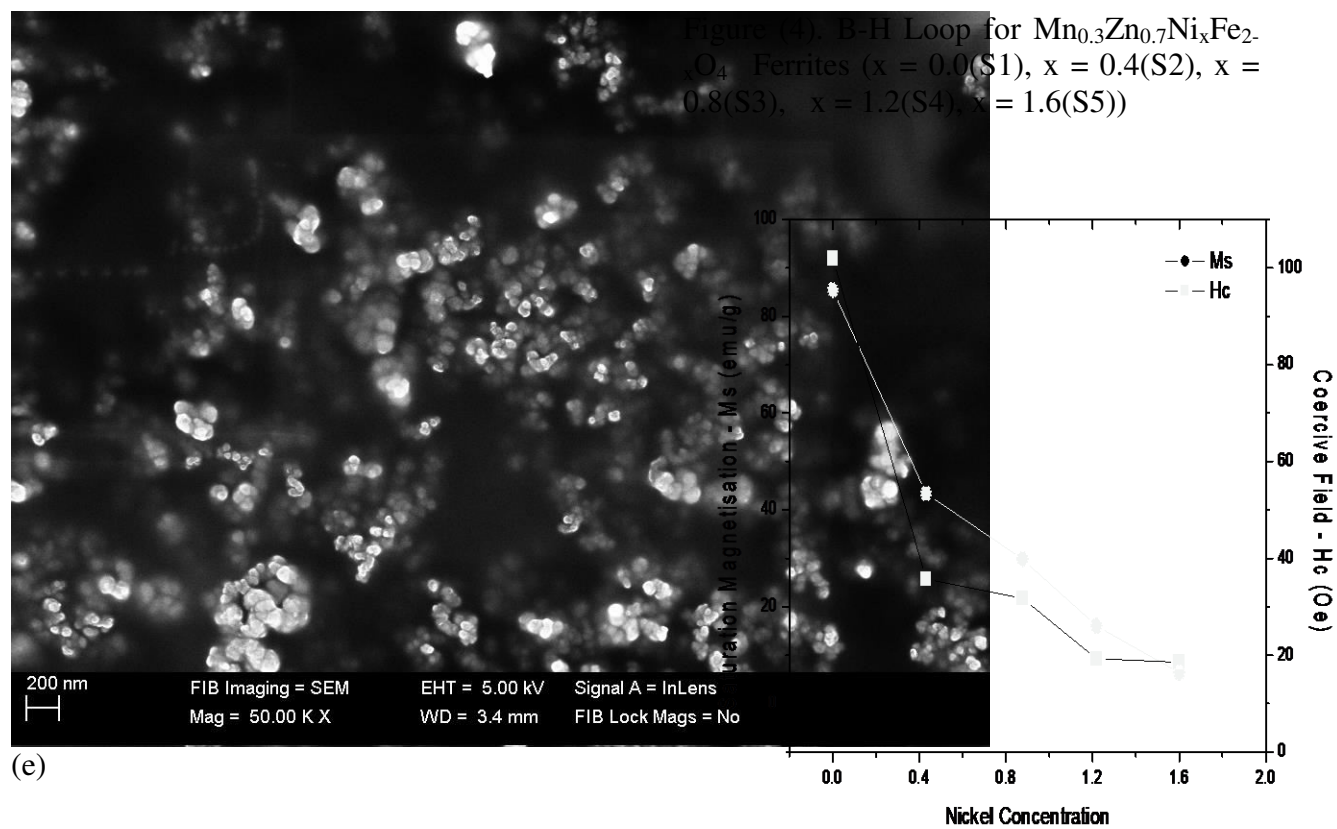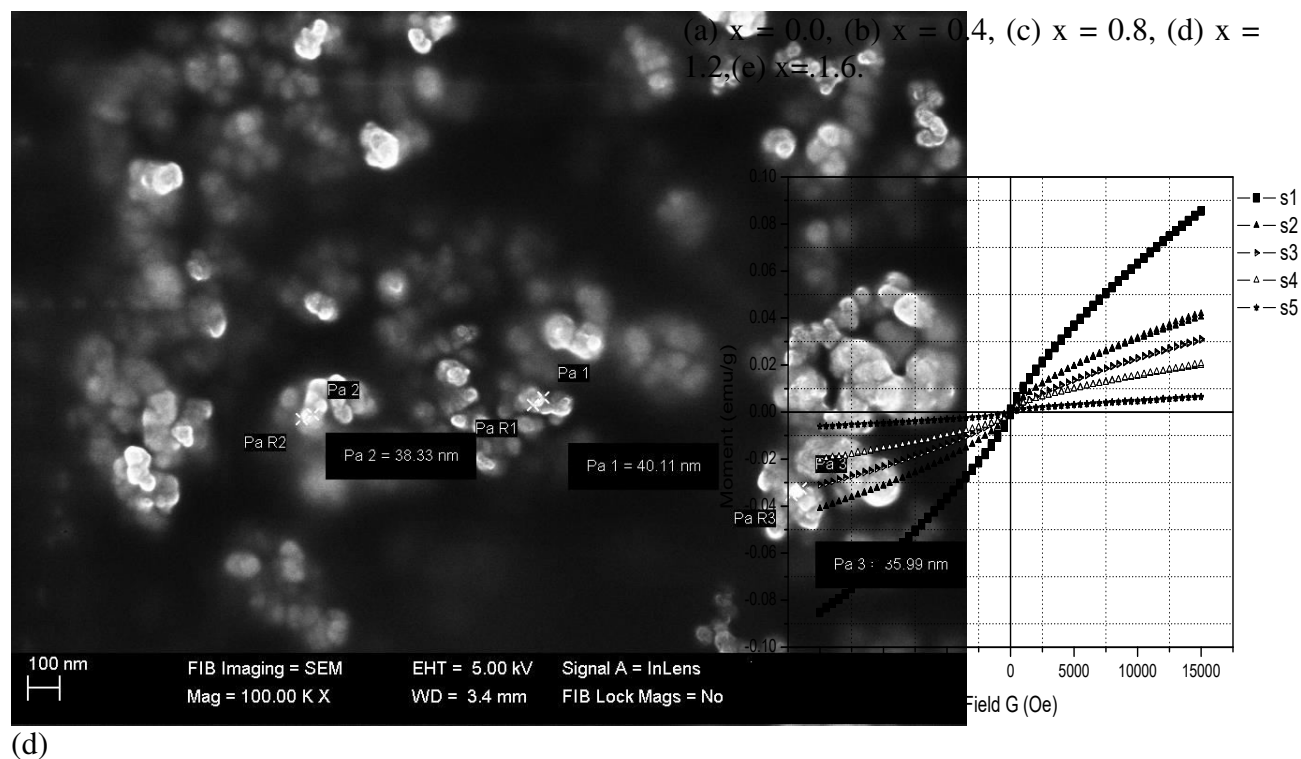
(e)

Figure (3). SEM Images of $Mn_{0.3}Zn_{0.7}Ni_xFe_{2-x}O_4$ Ferrites

Figure (5). Variation of Saturation Magnetisation and Coercive field with nickel concentration in $Mn_{0.3}Zn_{0.7}Ni_xFe_{2-x}O_4$ Ferrites.
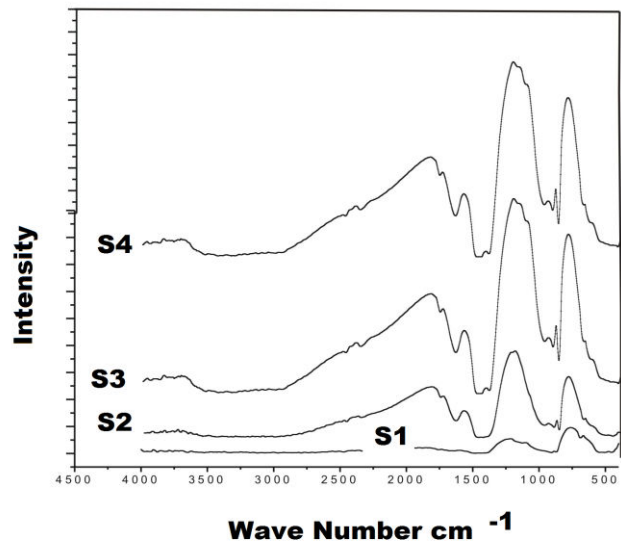

Figure (6). FTIR Spectra of $Mn_{0.3}Zn_{0.7}Ni_xFe_{2-x}O_4$ Ferrites.

References

[1] M.H. Sousa, F. Atourinho, J. Depeyrot, G.J. da Silva, M.C. Lara, J. Phys. Chem. B 105 (2001) 1168.

[2] K. Raj, R. Moskowitz, R. Casciari, J. Magn. Magn. Mater. 149 (1995) 174.

[3] T. Hyeon, Y. Chung, J. Park, S.S. Lee, Y.W. Kim, B.H. Park, J. Phys. Chem. B 6 (2002) 6831.

[4] R.V. Mehtha, R.V. Upadhyay, B.A. Dasanacharya, P.S. Goyal, K.S. Rao, J. Magn.

Magn. Mater. 132 (1994) 153.

[5] M.H. Kryder, Mater. Res. Soc. Bull. 21 (17) (1996) 184.

[6] D.G. Mitchell, J. Magn. Reson. Imaging 7 (1997) 1.

[7] P.P. Hankare, P.D. Kamble, S.P. Maradur, M.R. Kadam, U.B. Sankpal, R.P. Patil, K. Nimat, P.D. Lokhande, J. Alloys Compd. 487 (2009) 730.

[8] T. Mathew, K. Sreekumar, B.S. Rao, C.S. Gopinath, J. Catal. 210 (2002) 405.

[9] G. Blasse, Philips Res. Rept. (Netherlands) 20 (1965) 528.

[10] J.B. Goodenough, Magnetism and the Chemical Bond, John Wiley, New York, 1966.

[11] J. Smit, Magnetic properties of materials, in: Intra-University Electronics Series, vol. 13, 1971, p. 89.

[12] G.R. Dube, V.S. Darshane, Bull. Chem. Soc. Jpn. 64 (1991) 2449.

[13] V.A. Chaudhary, I.S. Mulla, K. Vihaymohanan, Sens. Actuators, B 55 (1999) 127.

[14]S.Maensiri, C.Masingboon, B.Boonchom, S.Seraphin, Acr.Mater.56(2007)797-800.

[15] M. George, A.M. John, S.S. Nair, P.A. Joy, M.R. Anantharaman, J. Magn. Magn. Mater. 302 (2006) 190.

[16] S. Giri, S. Samanta, S. Maji, S. Gangli, A. Bhaumik, J. Magn. Magn. Mater. 288 (2005) 296.

[17] S. Thompson, N.J. Shirtcliffe, E. O'keefe, S. Appleton, C.C. Perry, J. Magn. Magn. Mater. 292 (2005) 100.

[18] J. Wang, Mater. Sci. Eng., B 127 (2006) 81.

[19] A.S. Albuquerque, J.D. Ardisson, W.A.A. Macedo, J.L. Lopez, R. Paniago, A.I.C. Persiano, J. Magn. Magn. Mater. 226 (2001) 1379.

[20] P.P. Hankare, V.T. Vader, N.M. Patil, S.D. Jadhav, U.B. Sankpal, M.R. Kadam, B.K. Chougule, N.S. Gajbhiye, Mater. Chem. Phys. 113 (1) (2009) 233.

[21] P.P. Hankare, U.B. Sankpal, R.P. Patil, I.S. Mulla, P.D. Lokhande, N.S. Gajbhiye, J. Alloys Compd. 485 (2009) 798.

[22] S. Z. Zhang, G.L. Messing, J. Am. Ceram. Soc. 73 (1990) 61.

[23] J. Zhu, K.J. Tseng, IEEE Trans. Magn. 40 (5) (2004) 3339.

[24] S. M. Attia, Study of cation distribution of Mn-Zn Ferrites, Egypt. J. Solids. 29, 2 (2006)

[25] B. D. Cullity, In Elements of X-Ray diffraction, Addision-Wesley, London (1959) 325.

[26] I. N. Lin, R. K. Mishra,G. Thomas, IEEE Trans. Magn. MAG-20 (1) (1987) 134-139.

[27] A. Globus, J. Phys. (38) (1977) (C1) 15.

[28] A. C. Costa, E. Tortella, M. R. Morelli, R. H. Kiminami, Synthesis, Microstructure and magnetic properties of Ni-Zn ferrites,J.Magn.Magn.Mater.256 (2003) 174-182.

[29] P. Priyadharshini, A. Pradeep, P. S. Rao, G. Chandrasekarn, Material chemistry and physics, 116 (2009) 207-213.